human reproduction

ORIGINAL ARTICLE *Reproductive biology*

Localization and identification of sumoylated proteins in human sperm: excessive sumoylation is a marker of defective spermatozoa

Margarita Vigodner[1,4,*], Vibha Shrivastava[1], Leah Elisheva Gutstein[1], Jordana Schneider[1], Edward Nieves[2], Marc Goldstein[3], Miriam Feliciano[3], and Myrasol Callaway[2]

[1]Department of Biology, Stern College, Yeshiva University, 245 Lexington Avenue, New York, NY 10016, USA [2]Laboratory for Macromolecular Analysis & Proteomics, Albert Einstein College of Medicine, Bronx, NY, USA [3]515 East 71 St, Weil Medical College of Cornell University, Room-412, New York, NY 10021, USA [4]Department of Developmental and Molecular Biology, Albert Einstein College of Medicine, Bronx, NY, USA

*Correspondence address. Tel: +21–2–340-7769; Fax: +12-6-2-264-4294; E-mail:vigodner@yu.edu

BACKGROUND: Sumoylation is a type of post-translational modification that is implicated in the regulation of numerous cellular events. However, its role in the function of human sperm has not yet been characterized.

METHODS AND RESULTS: In this study, both immunofluorescence and electron microscopy revealed that small ubiquitin-like modifiers (SUMO) SUMO1 and SUMO2/3 were highly enriched in the neck area of human sperm that is associated with the redundant nuclear envelope and were also detectable in the flagella and some head regions. Similar localization patterns of SUMO were also observed in mouse and fly sperm. Nonmotile, two-tailed, curled tailed, misshapen, microcephalic (small head) and acephalic (no head) sperm exhibited abnormally high levels of sumoylation in their neck and tail regions relative to normal sperm. Numerous sumoylated proteins, ranging from 20 to 260 kDa, were detected via western blotting and identified by mass spectrometry, and 55 SUMO targets that were present specifically in human sperm, and not in the control fraction, corresponded to flagella proteins, proteins involved in the maturation and differentiation of sperm, heat shock proteins and important glycolytic and mitochondrial enzymes. The targets that were identified included proteins with specific functions in germ cells and sperm, such as heat shock-related 70-kDa protein 2, outer dense fiber protein 3, A-kinase anchor proteins 3 and 4, L-lactate dehydrogenase C, sperm protein associated with the nucleus on the X chromosome B/F, valosin-containing protein, seminogelins, histone H4 and ubiquitin. Coimmunoprecipitation experiments confirmed the sumoylation of semenogelin and indicated that some sperm proteins are modified by sumoylation and ubiquitination simultaneously.

CONCLUSIONS: Numerous proteins are modified by sumoylation in human sperm; excessive sumoylation is a marker of defective spermatozoa.

Key words: sperm / sumoylation / redundant nuclear envelope / defective spermatozoa / ubiquitin

Introduction

Spermatogenesis in the testis produces testicular sperm that undergo additional maturation in the epididymis. Final sperm activation occurs in the female reproductive tract via a process known as capacitation, which involves both reorganization of the sperm plasma membranes and alterations in flagellar beating patterns (Visconti et al., 1995a; Visconti et al., 1995b). Successful progression through sperm maturation and activation is crucial for normal fertilization. Unfortunately, the production of abnormal sperm, which is rather common in humans, may result in infertility, spontaneous abortion or birth defects. Although recent studies have provided important new data about the mechanism of sperm maturation, the underlying cause of most male infertility cases has yet to be identified. Therefore, addressing the etiology of infertility requires a better understanding of molecules such as proteins and their novel post-translational modifications (PTMs) in sperm.

PTMs occur after proteins are synthesized. Sperm are highly dependent on different types of PTMs since their transcriptional

machinery is inactive. The PTM of phosphorylation has been extensively studied in sperm and has been shown to regulate multiple processes, including motility and capacitation (Visconti, 2009). Numerous human sperm proteins have also been identified as targets of nitrosylation (Lefievre et al., 2007). Protein ubiquitination has also been detected in several regions of human sperm and is initially inversely related to semen quality (Sutovsky et al., 2001). Other studies have suggested that ubiquitination also plays a role in normal sperm function (Sutovsky, 2003; Muratori et al., 2005; Haraguchi et al., 2007).

Another type of PTM by small ubiquitin-like modifiers (SUMO) has emerged as an important regulatory mechanism in germ cells. There are three major isoforms of SUMO proteins in mammals: SUMO1, SUMO2 and SUMO3. SUMO2 and 3 are 95% identical and are often referred to as SUMO2/3 (Gill, 2005; Geiss-Friedlander and Melchior, 2007; Hannoun et al., 2010; Wilkinson and Henley, 2010). We, as well as others, have localized SUMO to different subcompartments of mouse and human testicular cells (Rogers et al., 2004; Vigodner and Morris, 2005; Vigodner et al., 2006; Shrivastava et al., 2010) and, during the course of the current study, another group has reported that SUMO1 is localized mostly to the heads of human sperm (Marchiani et al., 2010). These authors also found an inverse correlation between sumoylation and progressive cell motility, which however could not be explained by their reported localization. Western blots from the same study identified only three major SUMO-positive bands, and their published data did not provide any information about the localization and expression pattern of SUMO2/3. Importantly, targets of sumoylation have not been identified, although such targets are critical for understanding the role of SUMO in normal and impaired sperm function. Furthermore, SUMO proteins are highly conserved through evolution, but it is unknown whether they are detectable in the sperm of other species.

In this study, we provide new data describing the localization of SUMO1 and SUMO2/3 in sperm from humans and other species. In addition to its reported head localization, both SUMO1 and SUMO2/3 were highly enriched in the neck area of sperm, were associated with the redundant nuclear envelope (RNE) and were also detectable along the whole length of the sperm flagella. A similar SUMO localization pattern was detected in mouse and fly sperm. Nonmotile, misshapen, cephalic (small head) and aciphalic (no head) sperm had significantly higher levels of sumoylated proteins relative to their normal counterparts. Multiple sumoylated proteins were also detected via western blots. Mass spectrometric analysis specifically identified 55 SUMO targets in sperm, including major flagella proteins, proteins involved in sperm maturation and differentiation, heat shock proteins and important glycolytic and mitochondrial enzymes.

Materials and Methods

Reagents and antibodies

A rabbit polyclonal antibody against SUMO2/3 (ab3742 lot 721002 or 819168), a rabbit monoclonal against SUMO1 (ab32058), a rabbit polyclonal against ubiquitin (ab7780), a rabbit polyclonal against semenogelin II (ab47141) and a monoclonal antibody against nuclear pore complex (Mab414, ab24609) were purchased from Abcam (Cambridge, MA, USA). Mouse G10 Platinum anti-phosphotyrosine antibody was from Millipore (05-1050; Temecula, CA, USA). All remaining reagents were purchased from Sigma (St. Louis, MO, USA) unless otherwise noted.

Human sperm

Sperm samples were obtained from the male fertility clinic at the Weill Cornell College of Medicine of Cornell University in New York City. Informed consent was obtained from all patients in accordance with the protocol approved by the Institutional Review Board of the Weill Cornell Medical College. Semen samples were obtained by masturbation after 3–5 days of sexual abstinence and were subjected to a routine seminal analysis of volume, sperm concentration, total sperm number per ejaculate, motility, vitality and normal morphology according to the criteria of World Health Organization (WHO, 1999). There were 10 normal samples and 40 samples with decreased motility and/or morphology parameters used in this study.

The human specimens that were received for the experiments did not contain any code derived from individual personal information.

The samples were separated on PureSperm gradient (Nidacon, Mölndal, Sweden) according to the manufacturer's instructions. Depending on the experiment, 95, 80, 57 or 40% fractions were used. The fractions were pelleted and washed with 1 ml of human tubal fluid (HTF) medium (Irvine Scientific, Santa Ana, CA, USA) and centrifuged at 700 g for 10 min.

For some experiments, motile sperm fractions from normal donors were used to induce in vitro capacitation. Sperm pellets consisting of $\sim 3 \times 10^6$ cells were resuspended in 1.5 ml of HTF that was supplemented with human serum albumin (HAS, 5 mg/ml final concentration) and $NaHCO_3$ (10 mM final concentration) and incubated for 4 h at 37°C in 5% CO_2. The control sample was incubated without the addition of human serum albumin HSA and $NaHCO_3$. The sperm were pelleted and washed with 1 ml of HTF at 700 g for 10 min.

Protein extraction and western blot analysis of SUMO expression

For each condition, pellets of $\sim 3 \times 10^6$ sperm were resuspended in 80 μl of 2× Laemmli buffer [126 mM of TRIS/HCl, 20% Glycerol, 4% sodium dodecyl sulfate (SDS)] and boiled for 5 min at 100°C. After boiling, the samples were centrifuged for 2 min, and the supernatants were collected in fresh Eppendorf tubes. Protein concentrations were determined via a bichromic acid protein assay using bovine serum albumin (BSA) as the standard (Pierce, Rockford, IL, USA). Before running the samples, β-mercaptoethanol was added at 5% and bromphenolblue at 0.02% of the sample volume and the samples were boiled again for 3 min.

To prepare Triton X-100 soluble and insoluble fractions, sperm pellets were resuspended in 60 μl of a 1% Triton X-100 solution supplemented with protease inhibitor cocktail (Sigma) and the isopeptidase inhibitor N-ethylmaleimide (NEM; 25 mM), which prevents the cleavage of SUMO from modified proteins. After 15 min of extraction on ice, samples were centrifuged for 2 min. The supernatant (i.e. the triton-soluble fraction) was combined with 60 μl and the pellet (i.e. the triton-insoluble fraction) was resuspended in 120 μl of 2× Laemmli buffer. The samples were boiled for 5 min at 100°C and then supplemented with β-mercaptoethanol, as described above, prior to gel electrophoresis.

Gel electrophoresis was performed under reducing conditions using NuPAGE 4–12% gradient Bis-Tris polyacrylamide gels and MOPS running buffer (Invitrogen, Carlsbad, CA) at a constant 200 V. After electrophoresis, the proteins were transferred to a nitrocellulose membrane (0.45 μm, Invitrogen, Carlsbad, CA, USA) using NuPAGE transfer buffer. Protein electrophoresis and transfer were performed with an Invitrogen XCell SureLock Mini-Cell electrophoresis system. Western blotting was performed using the ECL plus kit (GE Healthcare, Piscataway, NJ, USA) in accordance with the manufacturer's instructions. SUMO1, SUMO2/3, semenogelin and ubiquitin antibodies were used at 1:500

dilutions, and antiphosphotyrosine was used at a 1:1000 dilution in PBS containing 1% BSA and 0.1% sodium azide. Equal loading was ensured with a monoclonal anti-β-tubulin antibody (1:2000; Abcam, ab7291). Quantitative analyses were performed using Quantity One software (Bio-Rad Laboratories, Hercules, CA).

Immunoprecipitation

Sperm protein lysates were centrifuged through an SDS-removal column (Pierce, Rockford, IL) prior to performing the immunoprecipitation (IP)

procedure. IP was performed using anti-SUMO antibodies and the Pierce Cross-link IP kit in accordance with the manufacturer's instructions.

Briefly, 10 μg of the SUMO2/3 antibody were crossed-linked to agarose beads, which were then incubated with 500 μg of proteins for 2 h at 4°C. Control resin beads that cross-linked with 4% agarose, supplied with the kit, were used without a cross-linked antibody to serve as a negative control for each experiment. After three washes with 200 μl of whole cell extraction buffer, which contained protease inhibitor cocktail and 20-mM NEM, the conjugated proteins were eluted with 50 μl of a glycine-based elution buffer (pH 2.8, supplied with the kit). The elution was
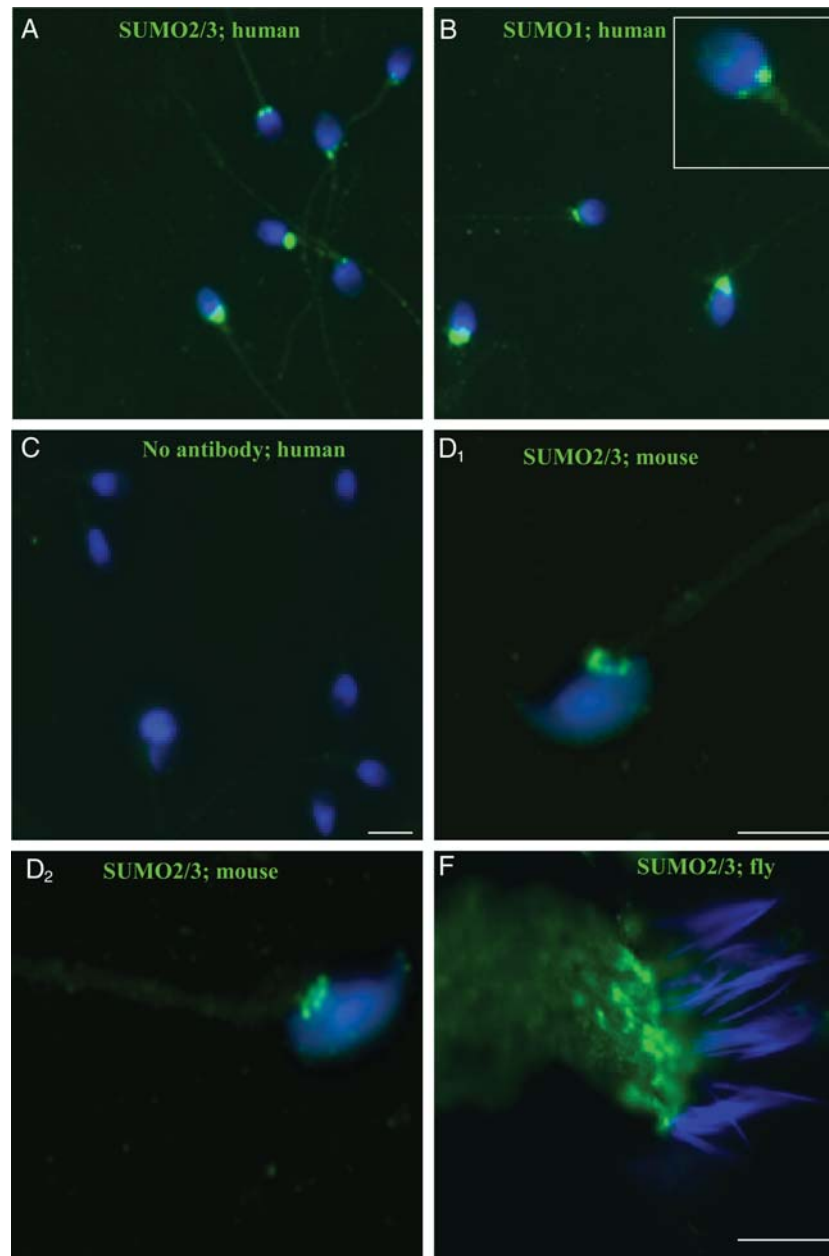

Figure 1 Localization of sumoylated proteins in human, mouse and fly sperm. (**A–C**) Immunofluorescent localization of SUMO2/3 (green, A) and SUMO1 (green, B) in human sperm. Neck and flagella regions are positively stained; the insert in B also shows positive staining in the sperm head region. Panel C shows a negative control with the omitted primary antibody. Chromatin is stained with DAPI (blue). (**D₁** and **D₂**) Localization of SUMO in mouse epididymal sperm. (**F**) Localization of SUMO in fly testicular sperm. The scale bar is 5 μm.

repeated two additional times. Western blot analysis with anti-SUMO antibodies was used to confirm IP.

Protein identification via gel staining, protein extraction and mass spectrometry

The eluted proteins were separated on a 4–12% gradient Bis-Tris NUPAGE gel for 5 min at 200 V. After electrophoresis, the gel was thoroughly washed with ultrapure water in a clean dish. The gel was then fixed for 15 min in a solution consisting of 50% methanol and 7% acetic acid and then washed twice with ultrapure water for 15 min. The gel was stained with GelCode Blue (Thermo Scientific, Waltham, MA, USA) for 1–2 h until bands became visible. The gel was then destained with ultrapure water for 1–2 h.

Mass spectrometry (MS) was performed with the assistance of the Laboratory for Macromolecular Analysis and Proteomics at the Albert Einstein College of Medicine of Yeshiva University and is described below.

First, Coomassie-stained cut protein gel bands were reduced with TCEP, alkylated with iodoacetamide and then digested with trypsin. The tryptic peptides were then desalted and concentrated with a C18 ZipTip (Millipore, Billerica, MA) and then diluted to 35 µl with a 0.1% formic acid aqueous solution (for a detailed description see Krasnikov et al., 2009).

Nanospray LC-MS/MS was performed with an Orbitrap Velos ultra-high-resolution mass spectrometer (Thermo Scientific) and the NanoAcquity UPLC system (Waters). The five most intense ions determined from an initial survey scan (300–1600 m/z; measured in the FT Orbitrap region at a resolution of 60 000 at m/z 400), with charge states of +2 or greater, were selected for fragmentation (MS/MS). MS/MS was performed with an isolation width of 2 m/z and a normalized collision energy of 35%. A minimum signal intensity of 1000 counts was required for triggering MS/MS. Dynamic exclusion was enabled, where once a certain ion is selected for MS/MS, this ion is excluded from subsequent selection during the next 90 s.

Raw data files were created with Proteome Discoverer 1.2, merged and searched against the human NCBI database (May 27, 2011) using the in-house Mascot Protein Search engine. The following search parameters were used: trypsin 2 missed cleavages; fixed modification of carbamidomethylation (Cys); variable modifications of deamidation (Asn and Gln), pyro-glu (Glu and Gln) and oxidation (Met); monoisotopic masses; peptide mass tolerance of 100 ppm, and product ion mass tolerance of 0.6 Da. Proteins were considered identified when having at least two unique bold red (BR; the most logical assignment of a peptide to a protein and prevents duplicate homologous proteins from being reported) significant peptides ($P \leq 0.05$).

Criteria for protein identification

Scaffold (version Scaffold_3_00_04, Proteome Software Inc., Portland, OR) was used to validate the peptides and proteins identified. Peptide identifications were accepted if they could be established at >95% probability as specified by the Peptide Prophet algorithm (Keller et al., 2002).
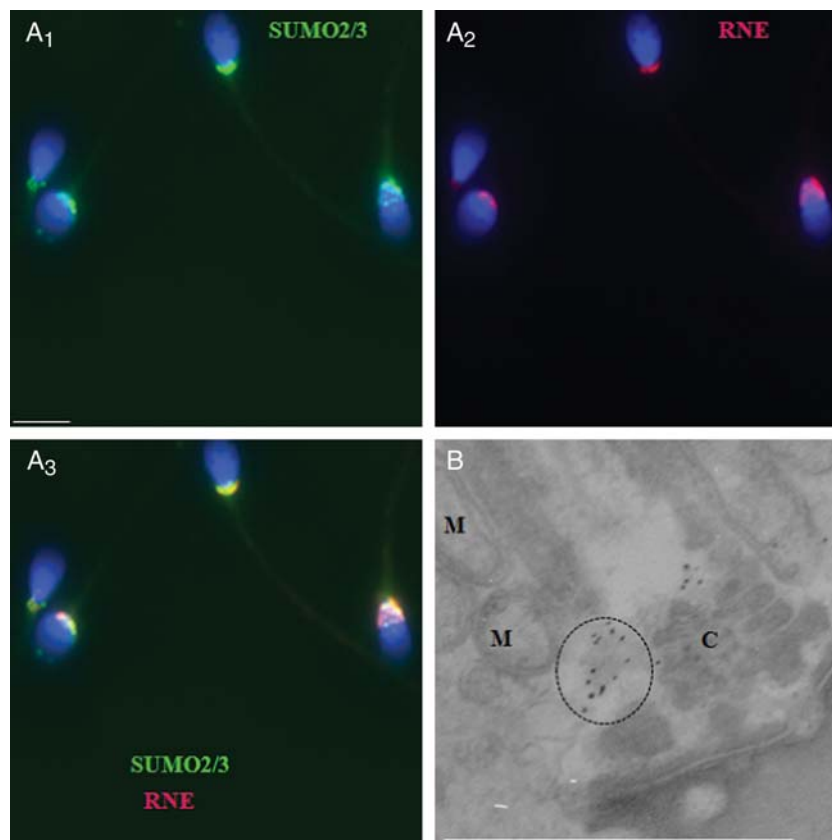

Figure 2 Sumoylated proteins are enriched in the region of the redundant nuclear envelope in human sperm. (A_1–A_3) SUMO2/3 (green) is significantly colocalized with an antibody against the nuclear pore complex (NPC, red), which serves as a marker of the redundant nuclear envelope (RNE) in human sperm. The scale bar is 5 µm. (**B**) Immunogold labeling of human sperm with an anti-SUMO2/3 antibody; positive staining in the neck area is highlighted by dashed circles. M, mitochondria; C, centriole.

Protein identifications were accepted if they could be established at >99% probability and contained at least two identified peptides. Protein probabilities were assigned by the Protein Prophet algorithm (Nesvizhskii *et al.*, 2003). After subtraction of common contaminants (such as keratins) and other nonspecifically eluted proteins, 55 of the 113 total proteins were found to be unique to the human sperm sample.

Fixation and immunofluorescence analysis

Mouse sperm were released from the cauda epididymis by mincing the tissue in PBS. Washed mouse and human sperm were attached to poly-lysine-coated slides. Slides with squashed fly testicles were obtained from the laboratory of Dr Tomer Avidor Reiss (Harvard Medical School). Slides were fixed in 1% paraformaldehyde and washed three times in PBS. Fixed cells on slides were treated for 10 min with 0.3% Igepal (NP-40) and preblocked for 30 min with Image-IT™ FX Signal Enhancer (Molecular Probes, Eugene, OR, USA). Cells were rinsed with PBS and incubated with either anti-SUMO1 or SUMO2/3 antibodies at final dilutions of 1:250 in PBS containing 1% BSA. The anti-semenogelin II antibody was used at 1:150 dilution. For colocalization studies, the cells were incubated in a mixture of anti-SUMO and either antinuclear pore complex (1:300) or antiphosphotyrosine (1:600) antibodies. Following one wash with PBS, the cells were incubated with Alexa Fluor 488-conjugated donkey anti-rabbit IgG (Molecular Probes) and/or Texas Red goat anti-mouse IgG (Vector Laboratories, CA, USA) at a 1:150 dilution in PBS containing 1% BSA. The cells were then washed three times, and the nuclei were stained for 5 min with 4 µg/ml of 4,6-diamino-2-phenylindole (DAPI). The samples were rinsed, and then the slides were mounted with a ProLong Antifade Kit (Molecular Probes). Images were collected with a Nikon inverted fluorescence microscope and 60× and 100× objective lenses with DAPI, fluorescein isothiocyanate and CY-5 filter sets. At least 50 cells were analyzed for each slide.

Immunogold labeling and transmission electron microscopy

Electron microscopy analysis was performed with the assistance of the Analytical Imaging Facility at the Albert Einstein College of Medicine of Yeshiva University.

Sperm were fixed on cover slips with 4% paraformaldehyde and 0.15% glutaraldehyde in 0.1-M sodium phosphate buffer for 30 min. They were then treated for 30 min with 50-mM glycine in PBS and permeabilized with 0.1% saponin. The cells were blocked with normal goat serum and incubated for 3–4 h with anti-SUMO antibodies at 1:100 final dilutions. The cells were then incubated for 1–2 h with a goat anti-rabbit ultra-small gold antibody (Aurion, Wageningen, The Netherlands) at a 1:100 dilution. After washing, the samples were postfixed in 2.0% glutaraldehyde in PBS, silver enhanced with Aurion R-GentSE_LM and dehydrated via a series of graded ethanol, after which the sample was embedded in LX112 resin (LADD Research Industries, Burlington, VT, USA). Ultrathin sections were cut on a Reichert Ultracut E ultramicrotome, stained with uranyl acetate and lead citrate and then viewed on a JEOL 1200EX transmission electron microscope at 80 kV.

Results

Immunofluorescence localization of SUMO in sperm

Immunostaining with anti-SUMO antibodies revealed a prominent signal in the neck area of human sperm. Higher exposure revealed that a faint, but specific, signal was observed along the whole length

of the flagella and in some sperm heads. A similar localization pattern was observed for both SUMO1 and SUMO2/3 antibodies (Fig. 1A and B: green fluorescence). In motile sperm from healthy donor samples, $91 \pm 5\%$ ($n = 10$) of the sperm were SUMO-positive in the neck, and $98 \pm 2\%$ ($n = 10$) were SUMO-positive in the tail, which suggested that this pattern of SUMO expression was a feature of normal spermatozoa. A signal in the head and/or acrosome signal (1B, insert) was only detectable in approximately half of the spermatozoa, $54 \pm 11\%$ ($n = 10$), which may have resulted from limited accessibility of the antibody or resolution of the microscope. The specificity of the signal was confirmed by using a secondary antibody alone followed by collection of images at the same level of fluorescence intensity (Fig. 1C).

To examine the possibility of SUMO expression in sperm from other species, mouse and fly sperm were also immunostained with anti-SUMO antibodies. Similar to human sperm, SUMO was enriched in the sperm neck area and was detectable along the tail; additionally, some sperm also exhibited a positive signal in their head and acrosome regions (Fig. 1D₁, D₂ and F).

Enrichment of sumoylated proteins in the redundant nuclear envelope

SUMO-positive regions in human sperm resembled a structure that has previously been described as a RNE, or nuclear pocket, which is formed as the nuclear envelope migrates to the sperm neck area during chromatin condensation and nuclear elongation (Haraguchi *et al.*, 2007). RNE has recently been implicated in several sperm functions, including Ca^{2+} storage, motility and protein turnover (Ho and Suarez, 2003; Westbrook *et al.*, 2006; Haraguchi *et al.*, 2007; Costello *et al.*, 2009; Ho, 2010). To test the possibility that SUMO associates
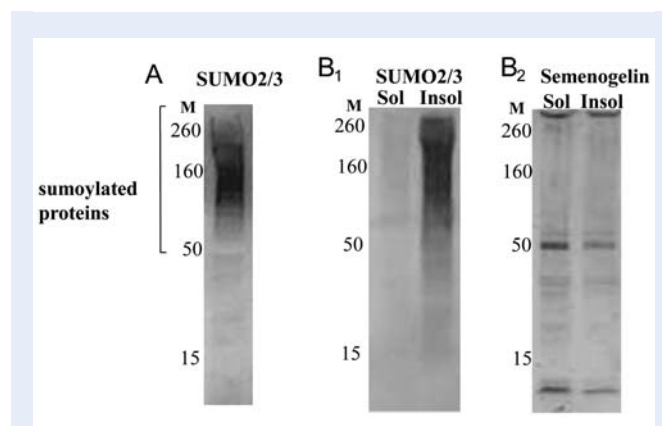

Figure 3 Expression pattern of sumoylated proteins in human sperm. Western blot analysis of SUMO2/3 expression following extraction of sperm proteins with SDS sample buffer at 100°C; SUMO conjugates of different molecular weights were detectable. (**A**) Migrating positions of molecular weight markers (M) are indicated. (**B₁** and **B₂**) Distribution of sumoylated proteins in Triton X-100-soluble (Sol) and -insoluble (Insol) fractions. The majority of the proteins are detected in the Triton X-100-insoluble fraction (B₁). The same membrane is also shown after incubation with an anti-semenogelin antibody (B₂).

with the RNE, coimmunolabeling was performed with anti-SUMO and antinuclear pore complex antibodies (NPC, which was previously used as a marker of RNE in sperm (Gibbs et al., 2010). The results of this analysis revealed a significant overlap of SUMO (Fig. $2A_1$, green fluorescence) and NPC (Fig. $2A_2$, red fluorescence), which resulted in a merged yellow-orange signal (Fig. $2A_3$). A closer analysis of the sperm neck area using an electron microscope confirmed that the SUMO-enriched regions correspond to the areas where RNE was previously localized (Westbrook et al., 2001) and are not centriole (C) or mitochondria (M). Similar results were obtained when SUMO1 (not shown) and SUMO2/3 antibodies were used.

Western blot analysis of sumoylated proteins in human sperm: extraction of Triton X-100-soluble and -insoluble protein fractions

Following the extraction of sperm proteins with SDS sample buffer at 100°C, anti-SUMO antibodies recognized multiple SUMO conjugates of different molecular weights on a western blot (Fig. 3A).

Triton X-100 extraction of sperm proteins (performed at 4°C) revealed that the majority of sumoylated proteins were detectable in the detergent-insoluble fraction, which is usually composed of cytoskeleton-associated proteins (Fig. $3B_1$). As a control for the experiment, the same membrane was incubated with an anti-seminogelin antibody. Seminogelin fragments of different molecular weights have previously been detected in both detergent-resistant and soluble fractions (de Lamirande and Lamothe, 2010). As expected, seminogelin fragments were detected at a comparable level in the two fractions (Fig. $3B_2$).

Comparative analysis of sumoylated proteins in normal and abnormal spermatozoa

Motile and nonmotile sperm fractions were prepared via density centrifugation of sperm samples from healthy donors and patients with abnormal sperm motility and/or morphology as per WHO (1999) criteria. For microscopic analysis, 80 or 95% PureSperm fractions were designated as motile and highly motile, respectively; similarly, the 40 and 57% fractions were designated as nonmotile and less-motile, respectively. Because some somatic cells were occasionally observed in the 40% fractions, western blot analysis was performed on the 57% fraction and the 95% fraction as less and highly motile sperm fractions, respectively. The 57% fraction was microscopically confirmed to be free of somatic cells.
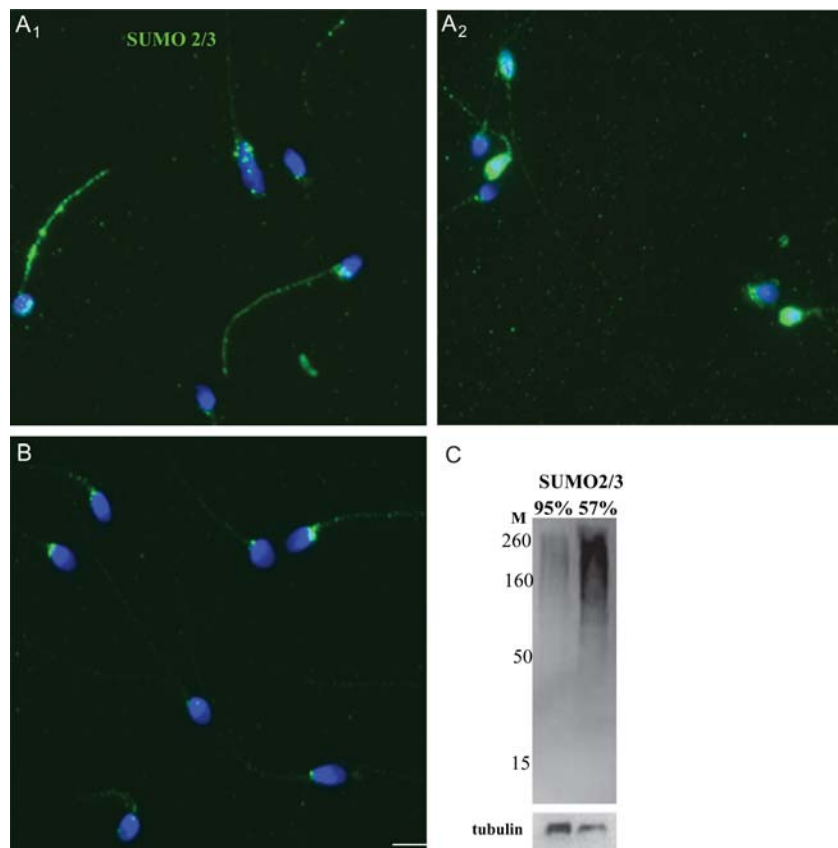

Figure 4 Comparative microscopic analysis of sumoylated proteins in normal and abnormal spermatozoa. (**A** and **B**) Representative images of SUMO expression in 40 and 57% PureSperm fractions (A_1 and A_2) relative to the 95% fraction (B). The fractions were obtained from a patient sample with decreased parameters for sperm motility and morphology. The scale bar is 5 μm. (**C**) A representative western blot image for 57 and 95% fractions is shown. Migrating positions of molecular weight markers (M) are indicated.

Microscopic analysis ($n = 40$) revealed a significantly higher level of sumoylation in the head, neck and tail regions of the sperm in the 40 and 57% fractions relative to the 80 and 95% fractions (Fig. 4A$_1$ and A$_2$ when compared with B; representative images are shown). Western blot analysis ($n = 6$) confirmed the significantly increased level of sumoylation in the 57% relative to the 95% fraction. For western blots, differences in the motile and immotile fractions from the same patient was assessed to avoid possible slight variability between the samples (Fig. 4C; a representative image is shown). Closer examination of the defective spermatozoa showed that sperm with two-tails and abnormal heads (Fig. 5A$_1$, A$_2$, B$_1$ and B$_2$) and sperm with curled tails (C$_1$ and C$_2$) were highly sumoylated. Another prominent and consistent feature was that acephalic (no head; D$_1$ and D$_2$) or microcefalic (small or pin head; E$_1$ and E$_2$; F$_1$ and F$_2$) spermatozoa were highly sumoylated in the head or neck and tail regions.

Induction of capacitation

After induction of *in vitro* capacitation, which was monitored by progressive phosphorylation of tyrosine residues of sperm proteins, no obvious changes in the overall localization of the sumoylated proteins could be visualized microscopically (Fig. 6A$_1$ and A$_2$). Western blot analysis revealed slight capacitation-induced changes in the intensity of some bands, but the response varied slightly among sperm samples from different normal donors. An increase in the level of tyrosine phosphorylation served as a positive control for the induction of capacitation (Fig. 6B$_1$ and B$_2$). Overall, no statistically significant increase or decrease in the global level of sumoylation occurred ($n = 8$), which suggests that the capacitation-induced changes, if they exist, must be studied using more sensitive techniques (e.g. at the level of individual SUMO targets or using 2D gels).

Identification of SUMO targets using mass spectrometry

The identification of SUMO targets is an important step toward gaining insight into the possible role of sumoylation in sperm. To this end, we extracted sperm proteins under denaturing conditions and then immunoprecipitated the protein lysates with anti-SUMO antibodies. The motile sperm fraction used for the analysis was from normal donors and was free of somatic cells (Fig. 7A). IP with a covalently cross-linked antibody minimized its presence in the eluted fraction and was beneficial for subsequent MS analysis. A sample was prepared and processed in parallel with the antibody sample by using control beads without a cross-linked antibody. Western blot analysis of the eluents confirmed the successful enrichment of sumoylated proteins, as well as minimal amount of proteins in
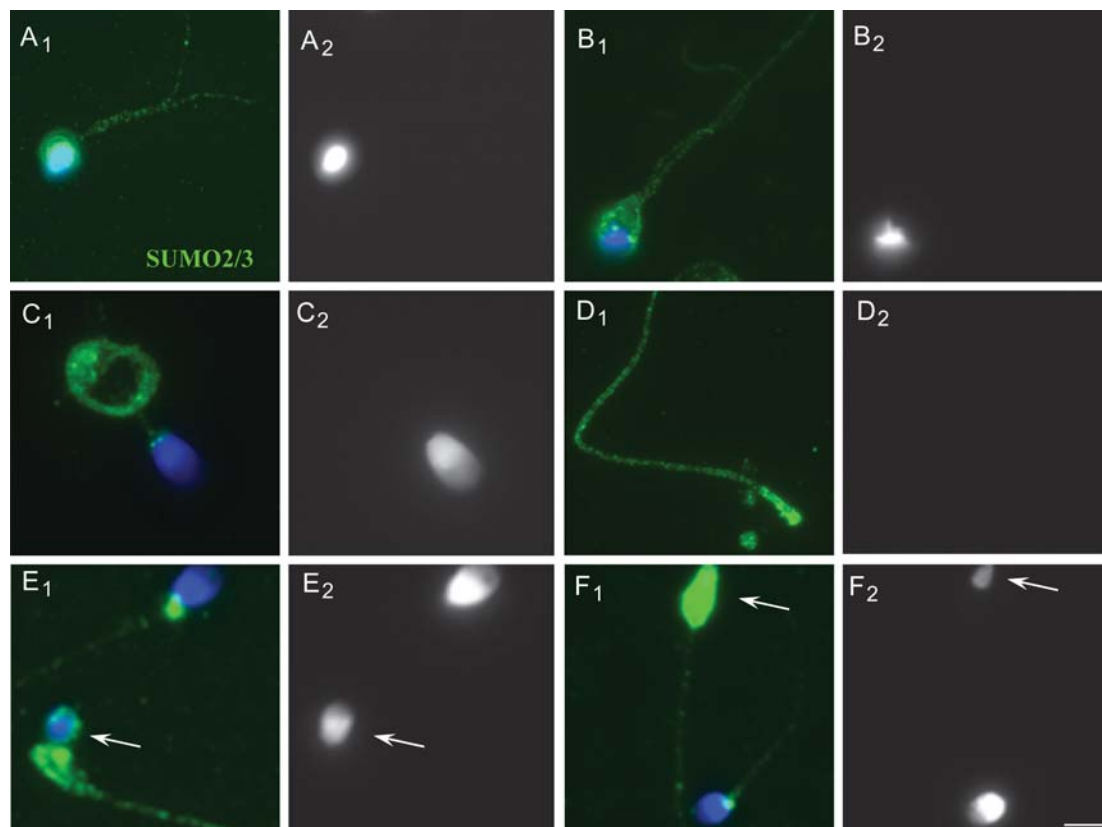

Figure 5 Localization of SUMO in human sperm with abnormal morphology. Immunofluorescent localization of SUMO (**A$_1$**–**F$_1$**) is shown alongside the corresponding DAPI images (**A$_2$**–**F$_2$**), which show the head morphology of the sperm. (A$_1$ and A$_2$; B$_1$ and B$_2$) Cells with two-tails and abnormal heads. (C$_1$ and C$_2$) A sperm with a banded tail. (D$_1$ and D$_2$) Acephalic (no head) sperm. (E$_1$ and E$_2$; F$_1$ and F$_2$) Microcefalic (small or pinhead, arrow) sperm. The scale bar is 5 μm.
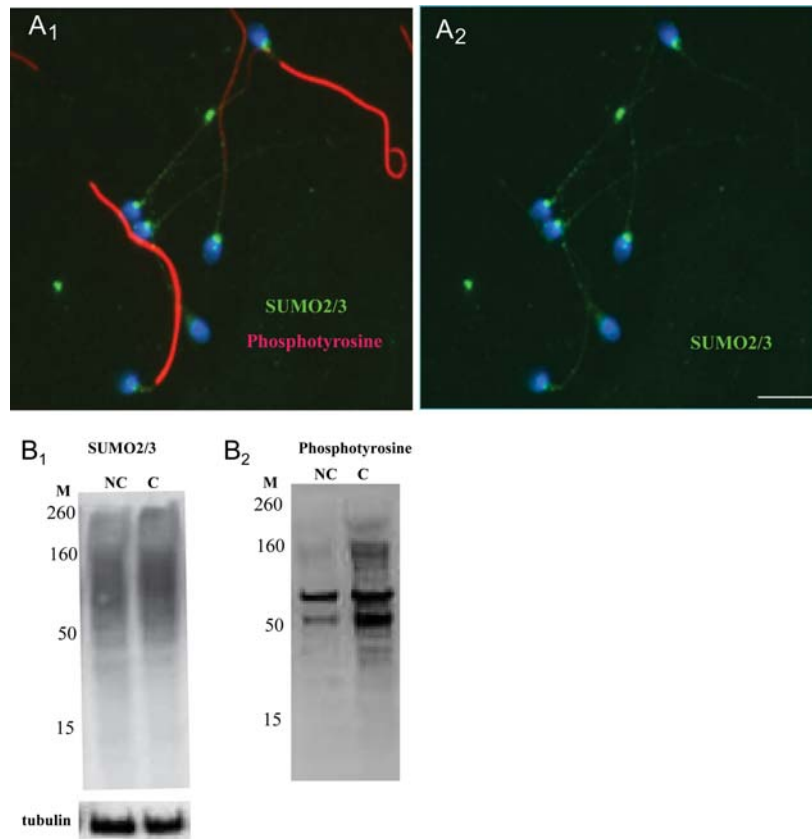
Figure 6 Sumoylated proteins in capacitated and noncapacitated spermatozoa. (**A₁** and **A₂**) Representative images of human sperm after an induction of *in vitro* capacitation. Capacitated spermatozoa are distinguished on the basis of massive tyrosine phosphorylation in their tails (red). No obvious microscopic changes were detectable in the SUMO localization pattern (green) on capacitation. The scale bar is 5 μm. (**B₁** and **B₂**) Western blot analysis of capacitated (**C**) versus noncapacitated (**NC**) human spermatozoa.

the negative control and flow-through fractions (Fig. 7B). The precipitated proteins were run on a gel for several minutes alongside the negative control samples, and the gel was fixed and stained (Fig. 7C). After protein digestion and MS analysis, 55 unique proteins to the antibody were identified when compared with the control (Table I). The identified SUMO targets were subdivided into several groups on the basis of their previously described functions in sperm (Ficarro *et al.*, 2003; Lefievre *et al.*, 2007; Secciani *et al.*, 2009; Baker *et al.*, 2010). The functional distribution of the proteins are as follows: proteins implicated in stress response and protein folding (18% of the total identified proteins), cytoskeletal and flagella proteins (22%), proteins previously implicated in sperm maturation, differentiation, acrosome reaction and cell–cell recognition (22%), glycolytic and mitochondrial enzymes (16%), and proteins involved in transcription, RNA-binding, translation and histones (22%, Fig. 7D). The identified targets included proteins with specific functions in germ cells and sperm, including heat shock-related 70-kDa protein 2, outer dense fiber protein 3, β-tubulin, A-kinase anchor protein 3 and 4, L-lactate dehydrogenase C, sperm protein associated with the nucleus on the X chromosome B/F, valosin-containing protein, ras-related protein Rab-2A, proacrosin binding protein sp32 precursor, acrosomal vesicle protein, seminogelins, histone H4, and ubiquitin.

Sumoylation and ubiquitination in human sperm

An interesting finding was that polyubiquitin was detected in the SUMO protein pull down. Ubiquitinated proteins have also been reported in the region of the RNE (Haraguchi *et al.*, 2007). IP with an anti-SUMO antibody, followed by a western blot with an anti-ubiquitin antibody (and vice versa), verified the MS findings. Although some ubiquitinated proteins could be detected in the SUMO-IP flow-through fraction, others were both ubiquitinated and sumoylated (Fig. 8).

Seminogelins are sumoylated in human sperm

Seminogelins have been implicated in several sperm functions and they localize to different regions in sperm, including the flagella. Coimmunoprecipitation experiments, followed by western blot analyses with SUMO and seminogelin-II antibodies, confirmed the sumoylation of different molecular weight fragments of seminogelin-II (Fig. 9). Immunofluorescent analysis confirmed the localization of seminogelin to the head, neck and tail regions of human sperm (Fig. 9).
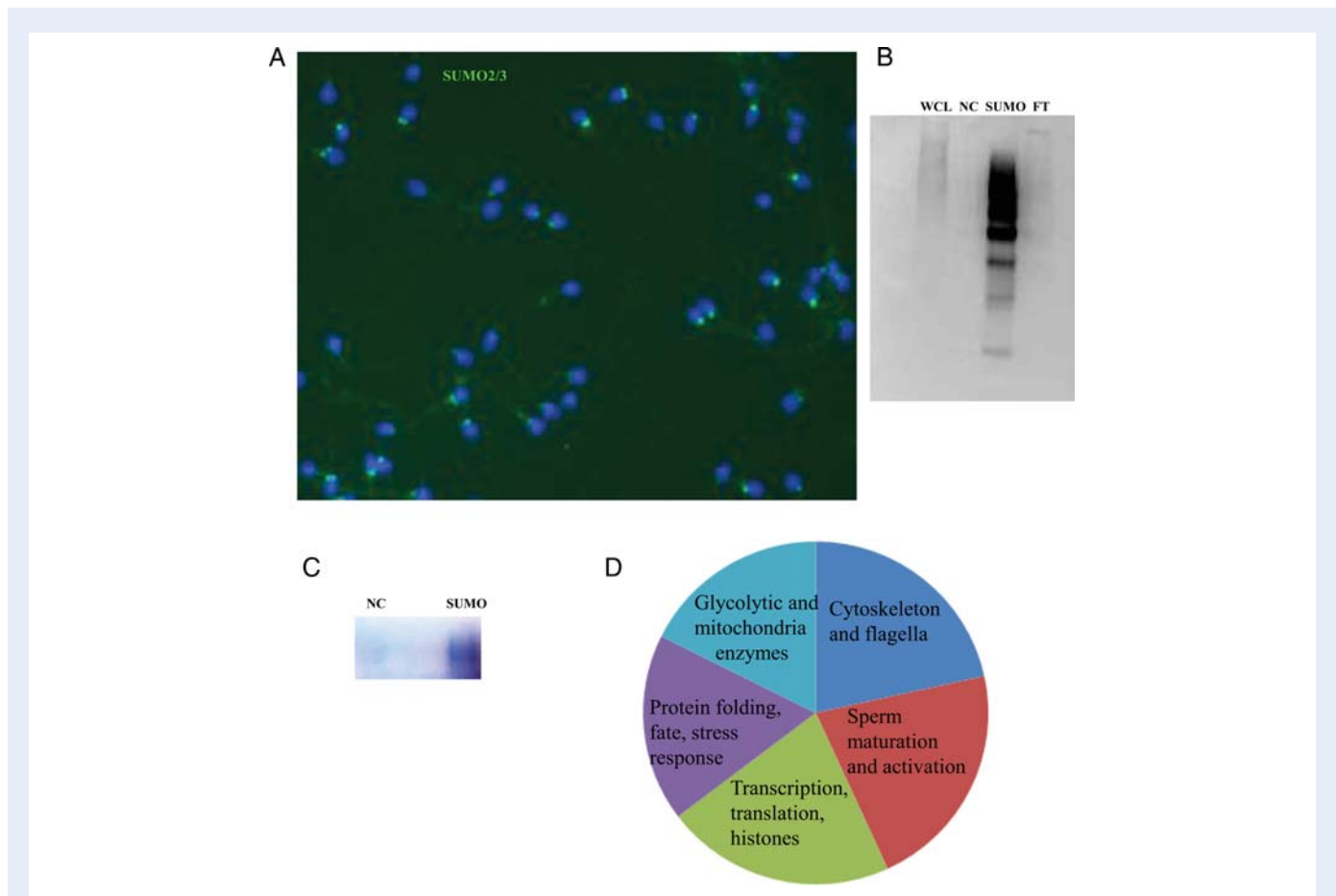
Figure 7 Identification of SUMO targets in human sperm. An image of a motile sperm fraction from a normal patient processed for mass spectrometry analysis. The sample has no somatic cells and shows a normal pattern of SUMO2/3 staining. (**A**) Western blot analysis of the sample after immunoprecipitation with a SUMO2/3 antibody. Whole-cell lysate (WCL), negative control (NC), immunoprecipitated fraction (SUMO) and flow thorough (FT). (**B**) The negative control and the immunoprecipitated fractions are shown on a gel after fixation and staining, processing of the gel for protein digestion and mass spectrometry analysis. (**C**) Functional distribution of SUMO targets in human sperm.

Discussion

In this study, sumoylated proteins were localized to the neck, tail and head area of human sperm. Multiple sumoylated proteins ranging from 20 to 260 kDa were detected by western blot analyses. The localization of sumoylated proteins in different sperm regions was also supported by the results of the proteomic analysis, from which numerous head, flagella, and neck/RNE proteins were found to be sumoylated. Triton X-100 extraction of sperm proteins revealed that the majority of sumoylated proteins were detectable in the detergent-insoluble fraction, which is usually composed of cytoskeleton-associated proteins. In a similar manner, some of the identified targets (SPANX, AKAP3 and 4) have previously been identified in the triton-insoluble fraction, further supporting a possible association.

Somewhat differently from these results, a recent study of SUMO1 in human sperm (Marchiani *et al.*, 2010) showed only three major positive bands ranging from 50 to 80 kDa; this almost certainly resulted from insufficient sperm protein extraction without the use

of SDS and boiling. In our hands, nondenaturing treatment extracted only ~10–20% of the sumoylated proteins when compared with using SDS extraction and boiling. Localization studies from the same group reported the presence of SUMO1 in sperm heads. This might be explained by a permeabilization problem (Marchiani *et al.*, 2010). The authors suggested that some sperm might show a mitochondria signal. Our immunofluorescence and electron microscopy data clearly show that SUMO is enriched in the RNE and not the mitochondria; this pattern was obtained in almost 100% of normal sperm using different antibodies for SUMO1 and SUMO2/3 (as shown in the Fig. 1). Our data suggest that the two isoforms have the same expression pattern in human sperm. Similar SUMO localization patterns were detected in mouse and fly sperm, indicating that a possible evolutionarily conserved role of sumoylation in sperm function needs to be further studied. Indeed, SUMOs are highly conserved throughout evolution from yeast to mammals (Chosed *et al.*, 2006).

In their study, Marchiani *et al.*, 2010 used flow cytometry to describe an inverse correlation between the SUMO1 signal and progressive motility; however, this finding was difficult to explain in

Table 1 Identification of sumoylated proteins unique to the human sperm IP sample via tandem mass spectrometry.

Protein fate (folding, modification and turnover), stress response	# unique peptides	percent coverage	Protein Mol Wt (kDa)
gi|15010550 heat shock protein gp96 precursor [Homo sapiens]	6	11	90.2
gi|119620390 chaperonin containing TCP1, subunit 4 (delta), isoform CRA_a [Homo sapiens]	2	6	52.5
gi|119582699 heat shock 70kDa protein 4, isoform CRA_b [Homo sapiens]	4	7	87.8
gi|306890 chaperonin (HSP60) [Homo sapiens]	2	6	61
gi|13676857 **heat shock-related 70 kDa protein 2 [Homo sapiens],**	2	15	70
gi|14250650 glutathione S-transferase mu 3 (brain) [Homo sapiens]	2	9	26.6
gi|2627129 polyubiquitin [Homo sapiens]	3	4	68.5
gi|48762932 t-complex protein 1 subunit theta [Homo sapiens],	5	11	59.6
gi|5453603 t-complex protein 1 subunit beta isoform 1 [Homo sapiens]	2	4	57.5
gi|119568002 t-complex 1, isoform CRA_b [Homo sapiens]	2	6	35.4
Cytoskeleton, flagella and cell movement			
gi|19526475 **outer dense fiber protein 3**	5	26	27.7
gi|116063573 filamin-A isoform 1	3	2	280
gi|194097350 alpha-actinin-1 isoform a [Homo sapiens], gi|94982457|gb|ABF50047.1| actinin alpha 1 isoform b [Homo sapiens]	4	6	105.6
gi|18088719 **tubulin, beta** [Homo sapiens]	3	23	49.7
gi|5031571 actin-related protein 2 isoform b [Homo sapiens]	3	10	44.8
gi|169218113 predicted: plakophilin-1-like, partial [Homo sapiens]	2	4	69.2
gi|112382250 spectrin beta chain, brain 1 isoform 1 [Homo sapiens],	2	1	274.6
gi|119608212 spectrin, alpha, non-erythrocytic 1 (alpha-fodrin), isoform CRA_b [Homo sapiens]	2	1	183.1
gi|119574932 vinculin, isoform CRA_a [Homo sapiens]	2	3	108.8
gi|28336 mutant beta-actin (beta'-actin) [Homo sapiens]	2	30	41.8
Protein kinaseA-anchoring proteins			
gi|119610330 **A kinase (PRKA) anchor protein 4**, isoform CRA_a [Homo sapiens] Phosphoryl	4	9	75.6
gi|21493041 **A-kinase anchor protein 3** [Homo sapiens]	3	5	94.8
Mitochondrial function			
gi|32189394 ATP synthase subunit beta, mitochondrial precursor	4	9	56.7
gi|40068518 6-phosphogluconate dehydrogenase, decarboxylating [Homo sapiens] PPP	2	6	53.1
gi|123228108 aconitase 2, mitochondrial [Homo sapiens],	3	4	87.8
gi|119590496 fumarate hydratase, isoform CRA_a [Homo sapiens]	2	8	52.7
Glycolysis			
gi|119600342 aldolase A, fructose-bisphosphate, isoform CRA_b [Homo sapiens]	3	13	39.8
gi|4504973 **L-lactate dehydrogenase C chain** [Homo sapiens construct]	3	11	36.3
gi|119619008 phosphoglycerate kinase 1, isoform CRA_a [Homo sapiens]	2	11	28.5
gi|13279239 ENO1 enolase 1, protein [Homo sapiens]	3	15	29.9
gi|119609192 glyceraldehyde-3-phosphate dehydrogenase, isoform CRA_a [Homo sapiens]	2	7	35.2
Sperm differentiation			
gi|111305821 **valosin-containing protein** [Homo sapiens] Phosphoryl	3	5	89.3
gi|4506365 ras-related protein Rab-2A	4	25	23.5
gi|13366086 proacrosin binding protein sp32 precursor [Homo sapiens], gi|119609180|gb|EAW88774.1| acrosin binding protein [Homo sapiens]	2	5	61.4
gi|119614801 clathrin, heavy polypeptide (Hc), isoform CRA_a [Homo sapiens]	2	1	192.4
gi|119574079 guanine nucleotide binding protein (G protein), beta polypeptide 2-like 1, isoform CRA_c [Homo sapiens]	2	7	42.9
gi|117938792 **SEMG1 protein** [Homo sapiens]	2	8	36.9
gi|117938793 **SEMG2 protein** [Homo sapiens]	2	14	34.3

Continued

Table I *Continued*

Protein fate (folding, modification and turnover), stress response	# unique peptides	percent coverage	Protein Mol Wt (kDa)
gi|119585171 lactotransferrin [Homo sapiens]	2	3	78.3
gi|222136622 prostate and testis expressed protein 3 precursor Acrosomal vesicle protein HEL-127;	2	15	11.7
gi|14196344 **sperm protein associated with the nucleus on the X chromosome B/F** [Homo sapiens],	2	27	11.8
Immunoglobilins			
gi|218783326 immunoglobulin heavy chain [Homo sapiens]	2	15	23.8
gi|113584 RecName: Full = Ig alpha-1 chain C region	2	7	37.7
Transcription, RNA-binding, Protein synthesis and Turnover			
gi|48734966 eukaryotic translation elongation factor 1 alpha 1 [Homo sapiens]	6	15	50.1
gi|119594432 eukaryotic translation elongation factor 1 gamma, isoform CRA_d [Homo sapiens]	4	8	48.4
gi|19353009 Similar to Elongation factor 2b [Homo sapiens]	4	13	57.5
gi|4503529 eukaryotic initiation factor 4A-I isoform 1 [Homo sapiens]	3	8	46.2
gi|119612222 poly(A) binding protein, cytoplasmic 1, isoform CRA_	4	12	47.3
gi|4758138 probable ATP-dependent RNA helicase DDX5 [Homo sapiens]	2	3	69.1
gi|55958183 ribosomal protein L7a [Homo sapiens]	2	13	21.5
gi|119627428 ribosomal protein S8, isoform CRA_a [Homo sapiens]	2	12	27.4
gi|315221152 60S ribosomal protein L11 isoform 1 [Homo sapiens], gi|15431290	2	13	20.1
gi|4504301 **histone H4** [Homo sapiens]	2	17	11.4
gi|33872272 RUVBL2 protein [Homo sapiens]	2	10	28
gi|55956919 heterogeneous nuclear ribonucleoprotein A/B isoform a [Homo sapiens]	2	8	36

Proteins of specific interest that are discussed in the 'Discussion' section are indicated in bold.

light of the reported head localization. Our results support and extend these data by providing visual evidence for excessive accumulation of SUMO in the neck, head and tail regions of non-motile and morphologically abnormal sperm. Defective spermatozoa with curled tails, two tails, and abnormal head shapes could easily be distinguished from their normal counterparts by the abnormally high levels of sumoylation. A prominent feature of the microscopic analysis was that aciphalic or microcephalic sperm were heavily sumoylated in their neck and tail regions. These sperm could not be identified by flow cytometric analysis because they were nearly devoid of DNA; therefore, they were excluded from the earlier analysis (Marchiani *et al.*, 2010). It has been suggested that aciphalic spermatozoa arise from a combination of abnormal neck development during spermatogenesis and impaired development of the flagella in relation to the nucleus (Chemes *et al.*, 1999). SUMO proteins are highly expressed during spermatogenesis, and their possible role in formation of the abnormal phenotype in spermatids and sperm has to be further studied. Together, our data suggests that sumoylation may serve as an additional marker for defective spermatozoa during microscopic sperm analysis.

Similar to SUMO, excessive ubiquitination was detected on the surface of defective spermatozoa (Sutovsky, 2003). Our MS and coimmunoprecipitation experiments suggest that certain sperm proteins can be concomitantly modified by ubiquitination and sumoylation.

Numerous sumoylation targets identified in this study are directly involved in the regulation of sperm motility and function, for example tubulins, outer dense fiber protein 3 (ODF3 or SHIPPO), and A-kinase anchor protein 3 and 4 (AKAP3 and 4). Several glycolytic and mitochondria enzymes, including ATP synthase, were also identified as SUMO targets, which suggests that sumoylation may play a role in these two pathways of energy metabolism. Several stress-related proteins were additionally identified as SUMO targets, including two members of the heat shock protein 70 family (HSP70 proteins 2 and 4), HSP60, HSPgp96, glutathione s-transferase and several proteins of the chaperonin-containing TCP1 complex. Consistent with these findings, we recently demonstrated that sumoylation is involved in stress responses *in vivo* and *in vitro* in mouse testicular cells (Shrivastava *et al.*, 2010).

Seminogelins have been implicated in various sperm functions, including regulation of capacitation (de Lamirande and Lamothe, 2010). The sumoylation of seminogelins was confirmed in the present study via coimmunoprecipitation experiments. Similar to SUMO, seminogelin is detectable in the tail, neck and head regions of sperm.

We could not visualize a significant re-localization of SUMO or changes in global sumoylation following capacitation; however, sumoylation and/or desumoylation of a specific target is likely below the
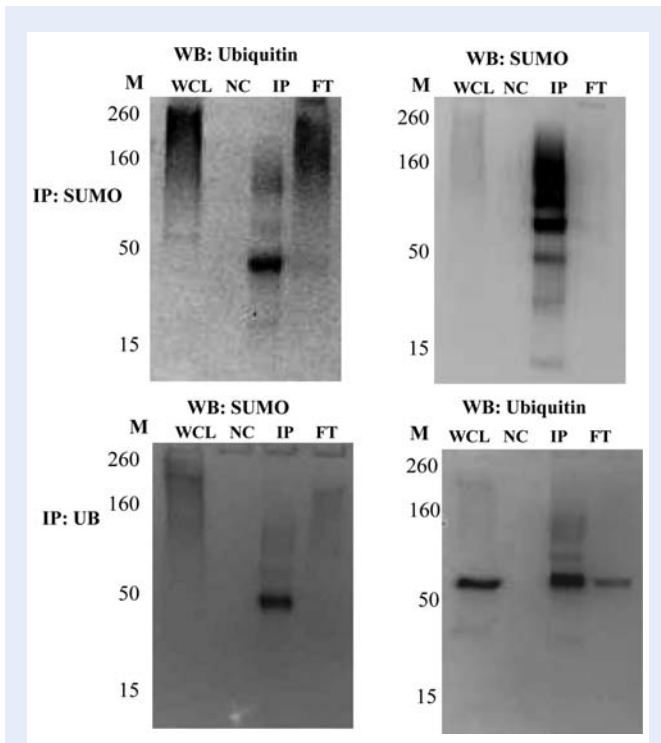
Figure 8 Coimmunoprecipitation of sumoylated and ubiquitinated proteins in human sperm. Immunoprecipitations (IP) using SUMO or ubiquitin antibodies followed by western blotting (WB) with the indicated antibodies are shown. Whole-cell lysate (WCL), negative control (NC), immunoprecipitated fraction (IP) and flow thorough (FT) are shown.

resolution limit of a microscope and, therefore, should be studied with other techniques.

Similar to several previous proteomic studies, we identified proteins involved in transcription and translation in ejaculated spermatozoa. Our sample was free of somatic cells, as shown in Fig. 7A, indicating that these proteins may remain in sperm after functioning in the previous stages of sperm maturation and then be localized to cytoplasmic droplets; alternatively, they may have different specific functions in sperm.

The human sperm protein associated with the nucleus mapped to the X chromosome (SPAN-X) gene cluster is expressed in spermatids, spermatozoa and some tumors (Westbrook et al., 2001). The SPAN-X protein was identified as a SUMO target in this study and has also been reported to specifically localized to the RNE (Westbrook et al., 2006), a finding that supports its possible sumoylation (Westbrook et al., 2006). Besides SPAN-X, several other proteins identified as SUMO targets (e.g. ubiquitin, VCP, semenogelin) are localized to the neck/RNE region. Although initially referred to as 'redundant', the RNE was recently implicated in several sperm functions (Ho and Suarez, 2003; Westbrook et al., 2006; Haraguchi et al., 2007; Costello et al., 2009; Ho, 2010). It has been suggested that, unlike other 'unwanted' components that are disposed of during sperm maturation, the RNE may play a role in sperm maturation and fertilization events. (Ho and Suarez, 2003; Costello et al., 2009). The SUMO signal in the RNE was very intense when compared with other sperm regions. It may be that normally only 5–10% of tail and head proteins are sumoylated and that 90% of the RNE proteins are sumoylated; a situation that would give a much brighter SUMO signal in the RNE. Indeed, our data with abnormal spermatozoa clearly show that the tail and midpiece proteins can be heavily sumoylated, but this is an abnormal situation. RNE can also be a domain in which different sumoylated proteins are recruited, similar to PML bodies for example.

It is important to note that several proteins identified in this study are also targets of tyrosine phosphorylation (Ficarro et al., 2003) and nitrosylation in sperm (Lefievre et al., 2007). The data further indicate the presence of complex interactions occurring between the different PTMs to regulate sperm function. Further studies will provide a better understanding of the relationship between secondary protein modifications and altered development/function. Unfortunately, many animal models are not informative and new ones need to be developed. For example, in mouse, consequences of SUMO1 deletion were most likely compensated for by SUMO2 and SUMO3 (Zhang et al., 2008). In a different manner, UBC9 (a SUMO-conjugating enzyme) -knockout mice show early embryonic lethality (Nacerddine et al., 2005)). Therefore, further optimization and improvement of sensitivity during MS analysis may in part contribute to our better understanding of protein post-translation modifications in sperm.

Authors' roles

M.V., V.S., L.E.G., and J.S. were responsible for planning and conducting of the experiments, writing and reading of the manuscript. E. N. and M.C. were responsible for mass spectrometry identification of sumoylated proteins, analysis of the results, writing and reading of the manuscript. M.G. and M.F. were responsible for collection and analysis of human sperm samples, analysis of the results of the study, writing and reading of the manuscript.
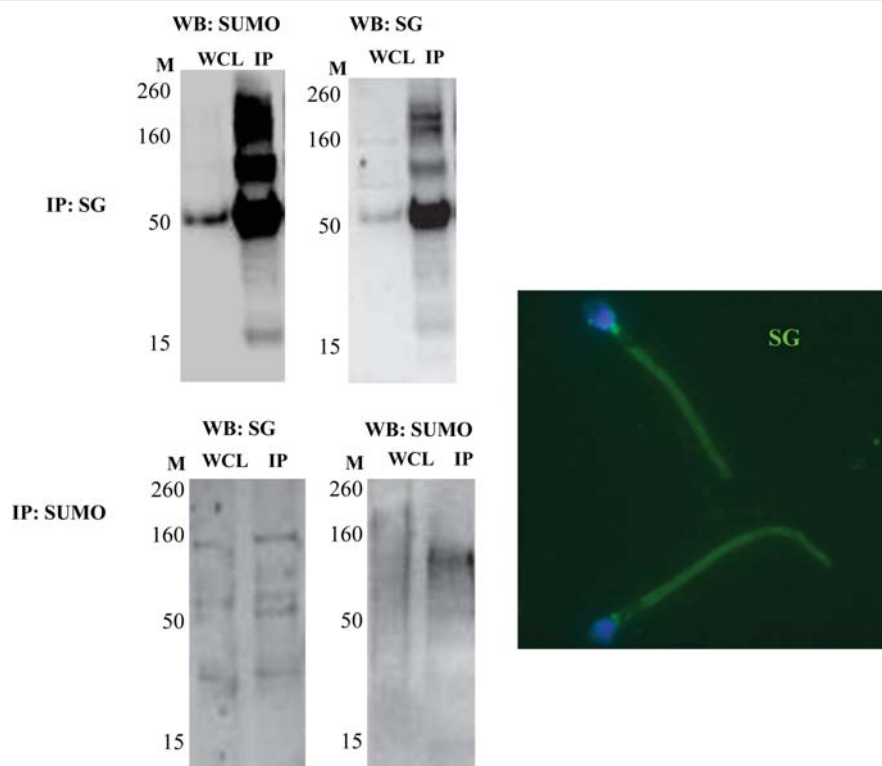
Conflict of interest

None declared.

Figure 9 Coimmunoprecipitation of SUMO and semenogelin in human sperm. Immunoprecipitations (IP) with SUMO or semenogelin II (SG) antibodies followed by western blot (WB) analyses with the indicated antibodies. Whole-cell lysate (WCL) and immunoprecipitated fractions (IP) are shown. The color image depicts the localization of semenogelin (green) in human sperm.

References

Baker MA, Reeves G, Hetherington L, Aitken RJ. Analysis of proteomic changes associated with sperm capacitation through the combined use of IPG-strip pre-fractionation followed by RP chromatography LC-MS/MS analysis. *Proteomics* 2010;**10**:482–495.

Chemes HE, Puigdomenech ET, Carizza C, Olmedo SB, Zanchetti F, Hermes R. Acephalic spermatozoa and abnormal development of the head-neck attachment: a human syndrome of genetic origin. *Hum Reprod* 1999;**14**:1811–1818.

Chosed R, Mukherjee S, Lois LM, Orth K. Evolution of a signalling system that incorporates both redundancy and diversity: Arabidopsis SUMOylation. *Biochem J* 2006;**398**:521–529.

Costello S, Michelangeli F, Nash K, Lefievre L, Morris J, Machado-Oliveira G, Barratt C, Kirkman-Brown J, Publicover S. Ca2+-stores in sperm: their identities and functions. *Reproduction* 2009;**138**:425–437.

de Lamirande E, Lamothe G. Levels of semenogelin in human spermatozoa decrease during capacitation: involvement of reactive oxygen species and zinc. *Hum Reprod* 2010;**25**:1619–1630.

Ficarro S, Chertihin O, Westbrook VA, White F, Jayes F, Kalab P, Marto JA, Shabanowitz J, Herr JC, Hunt DF et al. Phosphoproteome analysis of capacitated human sperm. Evidence of tyrosine phosphorylation of a kinase-anchoring protein 3 and valosin-containing protein/p97 during capacitation. *J Biol Chem* 2003; **278**:11579–11589.

Geiss-Friedlander R, Melchior F. Concepts in sumoylation: a decade on. *Nat Rev Mol Cell Biol* 2007;**8**:947–956.

Gibbs GM, Lo JC, Nixon B, Jamsai D, O'Connor AE, Rijal S, Sanchez-Partida LG, Hearn MT, Bianco DM, O'Bryan MK. Glioma pathogenesis-related 1-like 1 is testis enriched, dynamically modified, and redistributed during male germ cell maturation and has a potential role in sperm-oocyte binding. *Endocrinology* 2010; **151**:2331–2342.

Gill G. Something about SUMO inhibits transcription. *Curr Opin Genet Dev* 2005;**15**:536–541.

Hannoun Z, Greenhough S, Jaffray E, Hay RT, Hay DC. Post-translational modification by SUMO. *Toxicology* 2010;**278**:288–293.

Haraguchi CM, Mabuchi T, Hirata S, Shoda T, Tokumoto T, Hoshi K, Yokota S. Possible function of caudal nuclear pocket: degradation of nucleoproteins by ubiquitin-proteasome system in rat spermatids and human sperm. *J Histochem Cytochem* 2007;**55**:585–595.

Ho HC. Redistribution of nuclear pores during formation of the redundant nuclear envelope in mouse spermatids. *J Anat* 2010; **216**:525–532.

Ho HC, Suarez SS. Characterization of the intracellular calcium store at the base of the sperm flagellum that regulates hyperactivated motility. *Biol Reprod* 2003;**68**:1590–1596.

Keller A, Nesvizhskii AI, Kolker E, Aebersold R. Empirical statistical model to estimate the accuracy of peptide identifications made by MS/MS and database search. *Anal Chem* 2002;**74**:5383–5392.

Krasnikov BF, Chien CH, Nostramo R, Pinto JT, Nieves E, Callaway M, Sun J, Huebner K, Cooper AJ. Identification of the putative tumor suppressor Nit2 as omega-amidase, an enzyme metabolically linked to glutamine and asparagine transamination. *Biochimie* 2009; **91**:1072–1080.

Lefievre L, Chen Y, Conner SJ, Scott JL, Publicover SJ, Ford WC, Barratt CL. Human spermatozoa contain multiple targets for protein S-nitrosylation: an alternative mechanism of the modulation of sperm function by nitric oxide? *Proteomics* 2007;**7**:3066–3084.

Marchiani S, Tamburrino L, Giuliano L, Nosi D, Sarli V, Gandini L, Piomboni P, Belmonte G, Forti G, Baldi E et al. Sumo1-ylation of human spermatozoa and its relationship with semen quality. *Int J Androl* 2010;**34**:581–593.

Muratori M, Marchiani S, Forti G, Baldi E. Sperm ubiquitination positively correlates to normal morphology in human semen. *Hum Reprod* 2005;**20**:1035–1043.

Nacerddine K, Lehembre F, Bhaumik M, Artus J, Cohen-Tannoudji M, Babinet C, Pandolfi PP, Dejean A. The SUMO pathway is essential for nuclear integrity and chromosome segregation in mice. *Dev Cell* 2005;**9**:769–779.

Nesvizhskii AI, Keller A, Kolker E, Aebersold R. A statistical model for identifying proteins by tandem mass spectrometry. *Anal Chem* 2003;**75**:4646–4658.

Rogers RS, Inselman A, Handel MA, Matunis MJ. SUMO modified proteins localize to the XY body of pachytene spermatocytes. *Chromosoma* 2004;**113**:233–243.

Secciani F, Bianchi L, Ermini L, Cianti R, Armini A, La Sala GB, Focarelli R, Bini L, Rosati F. Protein profile of capacitated versus ejaculated human sperm. *J Proteome Res* 2009;**8**:3377–3389.

Shrivastava V, Pekar M, Grosser E, Im J, Vigodner M. SUMO proteins are involved in the stress response during spermatogenesis and are localized to DNA double-strand breaks in germ cells. *Reproduction* 2010;**139**:999–1010.

Sutovsky P. Ubiquitin-dependent proteolysis in mammalian spermatogenesis, fertilization, and sperm quality control: killing three birds with one stone. *Microsc Res Tech* 2003;**61**:88–102.

Sutovsky P, Terada Y, Schatten G. Ubiquitin-based sperm assay for the diagnosis of male factor infertility. *Hum Reprod* 2001;**16**:250–258.

Vigodner M, Morris PL. Testicular expression of small ubiquitin-related modifier-1 (SUMO-1) supports multiple roles in spermatogenesis: silencing of sex chromosomes in spermatocytes, spermatid microtubule nucleation, and nuclear reshaping. *Dev Biol* 2005;**282**:480–492.

Vigodner M, Ishikawa T, Schlegel PN, Morris PL. SUMO-1, human male germ cell development, and the androgen receptor in the testis of men with normal and abnormal spermatogenesis. *Am J Physiol Endocrinol Metab* 2006;**290**:E1022–E1033.

Visconti PE. Understanding the molecular basis of sperm capacitation through kinase design. *Proc Natl Acad Sci USA* 2009;**106**:667–668.

Visconti PE, Bailey JL, Moore GD, Pan D, Olds-Clarke P, Kopf GS. Capacitation of mouse spermatozoa. I. Correlation between the capacitation state and protein tyrosine phosphorylation. *Development* 1995a;**121**:1129–1137.

Visconti PE, Moore GD, Bailey JL, Leclerc P, Connors SA, Pan D, Olds-Clarke P, Kopf GS. Capacitation of mouse spermatozoa. II. Protein tyrosine phosphorylation and capacitation are regulated by a cAMP-dependent pathway. *Development* 1995b;**121**:1139–1150.

Westbrook VA, Diekman AB, Naaby-Hansen S, Coonrod SA, Klotz KL, Thomas TS, Norton EJ, Flickinger CJ, Herr JC. Differential nuclear localization of the cancer/testis-associated protein, SPAN-X/CTp11, in transfected cells and in 50% of human spermatozoa. *Biol Reprod* 2001;**64**:345–358.

Westbrook VA, Schoppee PD, Vanage GR, Klotz KL, Diekman AB, Flickinger CJ, Coppola MA, Herr JC. Hominoid-specific SPANXA/D genes demonstrate differential expression in individuals and protein localization to a distinct nuclear envelope domain during spermatid morphogenesis. *Mol Hum Reprod* 2006;**12**:703–716.

Wilkinson KA, Henley JM. Mechanisms, regulation and consequences of protein SUMOylation. *Biochem J* 2010;**428**:133–145.

World Health Organisation. *WHO Laboratory Manual for the Examination of Human Semen and Sperm-Cervical Mucus Interaction*, 4th edn. Cambridge University Press, 1999.

Zhang FP, Mikkonen L, Toppari J, Palvimo JJ, Thesleff I, Janne OA. Sumo-1 function is dispensable in normal mouse development. *Mol Cell Biol* 2008;**28**:5381–5390.